



Article

Design of High-Dimensional Maps with Sine Terms

Othman Abdullah Almatroud¹, Viet-Thanh Pham², Giuseppe Grassi³, Mohammad Alshammari¹, Sahar Albosaily¹  and Van Van Huynh^{2,*} 

- ¹ Department of Mathematics, Faculty of Science, University of Ha'il, Ha'il 2440, Saudi Arabia; o.almatroud@uoh.edu.sa (O.A.A.); dar.alshammari@uoh.edu.sa (M.A.); s.albosaily@uoh.edu.sa (S.A.)
- ² Modeling Evolutionary Algorithms Simulation and Artificial Intelligence, Faculty of Electrical and Electronics Engineering, Ton Duc Thang University, Ho Chi Minh City 758307, Vietnam; phamvietthanh@tdtu.edu.vn
- ³ Dipartimento Ingegneria Innovazione, Università del Salento, 73100 Lecce, Italy; giuseppe.grassi@unisalento.it
- * Correspondence: huynhvanvan@tdtu.edu.vn

Abstract: The use of the advancements in memristor technology to construct chaotic maps has garnered significant research attention in recent years. The combination of memristors and nonlinear terms provides an effective approach to proposing novel maps. In this study, we have leveraged memristors and sine terms to develop three-dimensional maps, capable of processing special fixed points. Additionally, we have conducted an in depth study of a specific example (TDMM₁ map) to demonstrate its dynamics, feasibility, and application for lightweight encryption. Notably, our general approach could be extended to develop higher-dimensional maps, including four- and five-dimensional ones, thereby opening up the possibility to create numerous higher-dimensional maps.

Keywords: chaos; sine term; memristor; high dimension; discrete map; lightweight encryption

MSC: 39A33; 39A60; 65P20



Citation: Almatroud, O.A.; Pham, V.-T.; Grassi, G.; Alshammari, M.; Albosaily, S.; Huynh, V.V. Design of High-Dimensional Maps with Sine Terms. *Mathematics* **2023**, *11*, 3725. <https://doi.org/10.3390/math11173725>

Academic Editor: Zhouchao Wei and Liguo Yuan

Received: 31 July 2023

Revised: 27 August 2023

Accepted: 29 August 2023

Published: 30 August 2023



Copyright: © 2023 by the authors. Licensee MDPI, Basel, Switzerland. This article is an open access article distributed under the terms and conditions of the Creative Commons Attribution (CC BY) license (<https://creativecommons.org/licenses/by/4.0/>).

1. Introduction

A discrete map, also known as a discrete dynamical system, is a useful tool for the analysis of the behavior of chemical reactions and the spread of diseases [1]. Discrete maps can exhibit a variety of behaviors, including stability, periodicity, and chaos [2–5]. Fractional-order models and neural networks play a vital role in artificial intelligence and signal processing [6,7]. Discrete chaotic maps are particularly interesting because they exhibit complex and unpredictable behavior, even though they are deterministic and follow precise rules. Chaotic maps have important applications in fields such as cryptography, data encryption, and random number generation [8,9]. In this context, understanding and implementing the dynamics of discrete chaotic maps has become a crucial research topic [10,11].

The memristor is a fundamental electronic device that was proposed in 1971. However, it was not until 2008 that the first practical memristor was developed by a team of researchers at HP Labs. The development of the memristor has provided a new type of non-volatile memory that is faster, smaller, and requires less energy than existing technologies. Furthermore, memristors could be used in artificial intelligence, neuromorphic computing, and analog signal processing [12–14]. This has led to significant interest in the memristor from both the academic and industrial communities, with many researchers working to explore its full potential [15,16].

Memristors have been shown to be capable of generating chaotic behavior, and this property can be exploited to create new discrete chaotic maps [17–21]. Generally, authors explore 2D memristive maps due to their simplicity. However, recent research is also shifting towards investigating topics related to high-dimensional memristive maps, as they offer distinct advantages [22–24]. For instance, high-dimensional chaotic maps can

store and process significantly more information compared to low-dimensional maps. Wang et al. conducted a study on a 3D memristive Lozi map [22], while another research group reported on a bi-memristor map in [23]. Additionally, a comprehensive list of 3D maps with memristors was introduced [24]. Researchers remain highly intrigued by the quest for an effective approach to designing high-dimensional maps.

This work considers another way to build high-dimensional maps with memristors and sine terms. The following are the primary advancements of this study. This work introduces a highly efficient method for the creation of high-dimensional memristive maps. These maps exhibit two distinct types of special fixed points, a plane of fixed points and the absence of any fixed points, categorizing them as unique maps with hidden dynamics [25]. By applying an extension of the suggested approach, the generation of even more intricate higher-dimensional maps, including 4D and 5D maps, becomes conveniently achievable. In Section 2, the general model and four example maps are introduced. Section 3 focuses on the specific map (called TDMM₁). Further examples of high-dimensional maps are discussed in Section 4. Section 5 presents the conclusions.

2. Model of 3D Maps

Chaotic discrete maps have intrigued scientists for decades due to their unpredictable and complex behaviors. These systems find application in various fields, from cryptography and secure communications to chaotic circuit design. With the discovery of memristors, a new dimension was introduced to the understanding and exploration of chaos in discrete maps. Memristors, the fourth fundamental circuit element, possess unique properties that offer novel possibilities in chaotic dynamics research. Recently, different 2D memristive maps have been proposed [20,26,27]. However, a few higher memristive maps have also been reported [22–24]. In this work, we develop a model of 3D maps, as shown in Figure 1. The main parts of the model are a sine function $\sin(\cdot)$, a memristor, amplifiers (a_1, a_2, a_4, a_5), and a controller term a_3 . The sine function is a popular function that was first applied to develop special discrete maps. Exploring further, additional functions could be employed in constructing high-dimensional maps. The effect of the sine term is indicated by a_1 and a_4 . The memristor has an effect on the model through a factor a_2 , while a_5 represents the feedback from $x(n)$ to $z(n + 1)$. The term a_3 can be used to change the number of the model's fixed points.

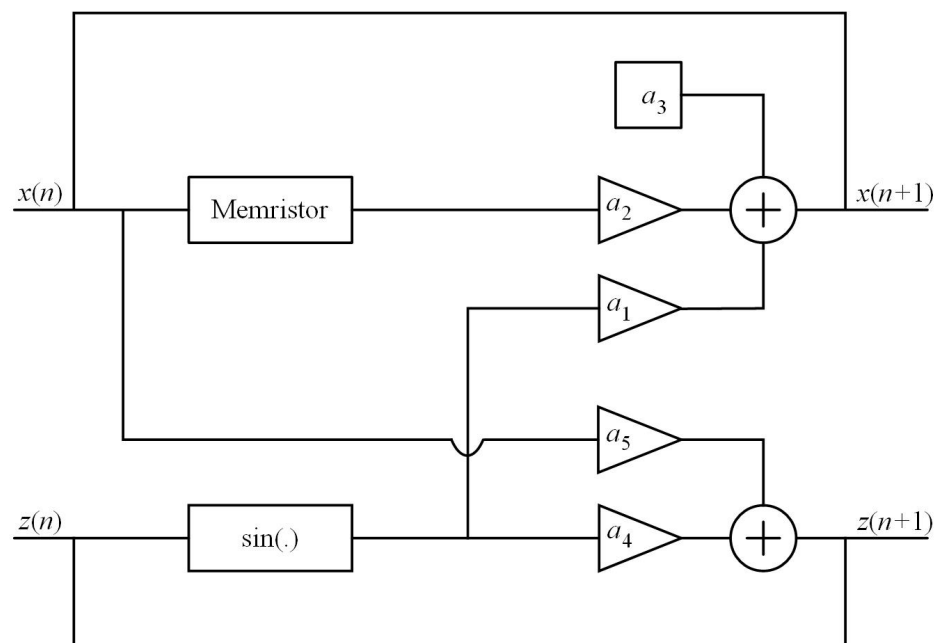


Figure 1. Diagram of 3D map using a sine function $\sin(\cdot)$ and a memristor.

From Figure 1, the mathematical model is derived as

$$\begin{cases} x(n+1) = a_1 \sin(z(n)) + a_2 M(y(n))x(n) + a_3 \\ y(n+1) = y(n) + x(n) \\ z(n+1) = a_4 \sin(z(n)) + a_5 x(n) \end{cases} \tag{1}$$

with discrete memristance $M(y(n))$ and parameters $a_i, i = 1, \dots, 5$. Here, x, y , and z are state variables. It is noted that x and z can be considered as the outputs of the model, while y is the internal state of the memristor.

The fixed point of (1) $P(x^*, y^*, z^*)$ is found by solving Equation (2)

$$\begin{cases} x^* = a_1 \sin(z^*) + a_2 M(y^*)x^* + a_3 \\ y^* = y^* + x^* \\ z^* = a_4 \sin(z^*) + a_5 x^* \end{cases} \tag{2}$$

We obtain

$$\begin{cases} x^* = 0 \\ \sin(z^*) = -\frac{a_3}{a_1} \\ z^* = -\frac{a_3 a_4}{a_1} \end{cases} \tag{3}$$

when $a_1 \neq 0$.

As shown in Equation (3), there is a plane of fixed points $P(0, y^*, 0)$ when $a_3 = 0$. When $a_3 \neq 0$, the fixed points depend on a_1, a_3 , and a_4 . In particular, the fixed points disappear for

$$\sin\left(\frac{a_3 a_4}{a_1}\right) \neq \frac{a_3}{a_1} \tag{4}$$

By selecting $M(y(n)) = (y(n))^2 - 1$, we obtain a three-dimensional memristive map (TDMM₁ map):

$$\begin{cases} x(n+1) = a_1 \sin(z(n)) + a_2 \left((y(n))^2 - 1 \right) x(n) + a_3 \\ y(n+1) = y(n) + x(n) \\ z(n+1) = a_4 \sin(z(n)) + a_5 x(n) \end{cases} \tag{5}$$

The TDMM₁ map is chaotic for

$$\begin{cases} a_1 = a_3 = a_4 = 0.1 \\ a_2 = 1.65 \\ a_5 = 1 \end{cases} \tag{6}$$

and $(x(0), y(0), z(0)) = (0.01, 0.01, 0.01)$ (see Figure 2a). The maximum Lyapunov exponent (MLE) equals 0.2697.

Selecting different memristors, it is possible to obtain new 3D maps based on the general model (1). In Table 1, we report new maps, while their chaotic dynamics are illustrated in Figure 2. While we exclusively present a singular set of parameter values for each map, it is important to note that there exist various parameter values leading to the chaotic behavior of these maps.

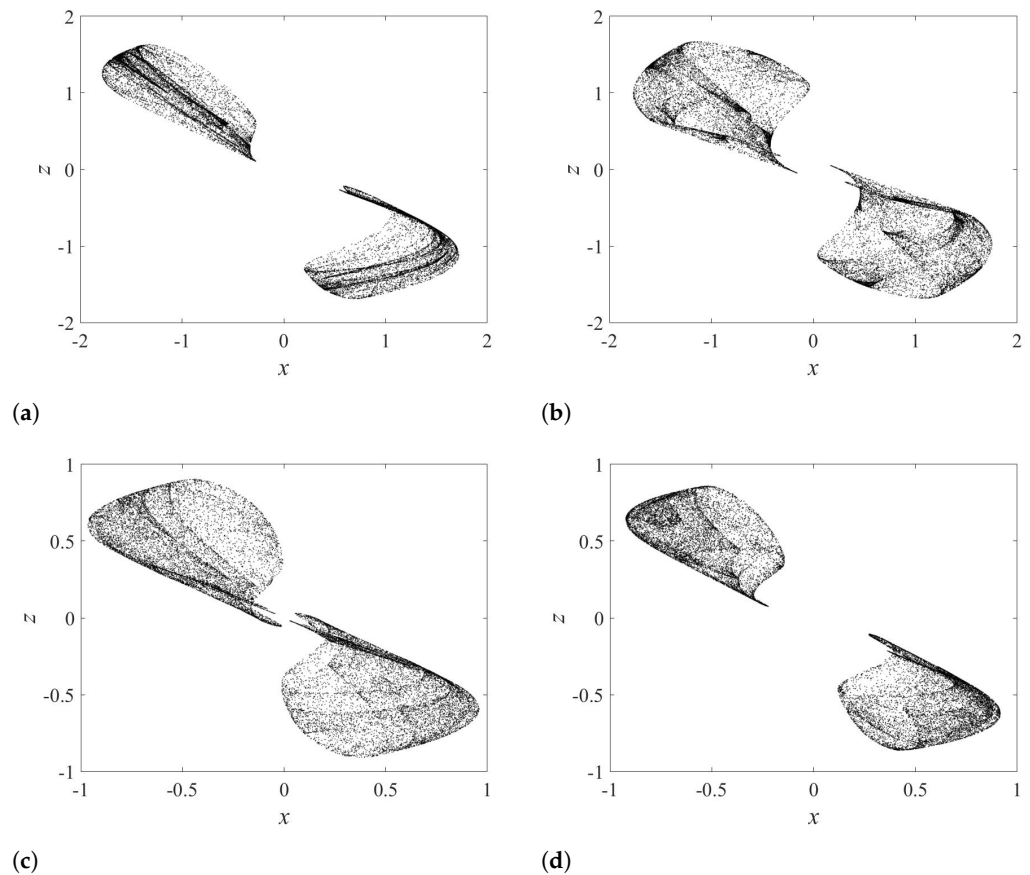


Figure 2. Iterative plots: (a) TDMM₁ map, (b) TDMM₂ map, (c) TDMM₃ map, (d) TDMM₄ map.

Table 1. List of new maps $(x(0), y(0), z(0)) = (0.01, 0.01, 0.01)$.

Name	Equations	Parameters	MLE
TDMM ₂	$x(n + 1) = a_1 \sin(z(n)) + a_2(y(n) - 1)x(n) + a_3$ $y(n + 1) = y(n) + x(n)$ $z(n + 1) = a_4 \sin(z(n)) + a_5x(n)$	$a_1 = a_4 = 0.1$ $a_2 = 2.3, a_3 = 0.01$ $a_5 = 1$	0.2046
TDMM ₃	$x(n + 1) = a_1 \sin(z(n)) + a_2 \sin(\pi y(n))x(n) + a_3$ $y(n + 1) = y(n) + x(n)$ $z(n + 1) = a_4 \sin(z(n)) + a_5x(n)$	$a_1 = a_4 = 0.1$ $a_2 = 1.8, a_3 = 0.01$ $a_5 = 1$	0.2415
TDMM ₄	$x(n + 1) = a_1 \sin(z(n)) + a_2(e^{-\cos(\pi y(n))} - 1)x(n) + a_3$ $y(n + 1) = y(n) + x(n)$ $z(n + 1) = a_4 \sin(z(n)) + a_5x(n)$	$a_1 = a_4 = 0.1$ $a_2 = 2.5, a_3 = 0.01$ $a_5 = 1$	0.214

3. Study of TDMM₁ Map

The TDMM₁ map (5) has no fixed point when $a_1 = a_3 = a_4 = 0.1$ and $a_5 = 1$. We consider the effect of the memristor on the dynamics by changing a_2 from 1.3 to 1.7 (see Figure 3). Both chaotic and non-chaotic behaviors are observed in this range of a_2 . Figure 3a shows a route from periodic dynamics to chaos.

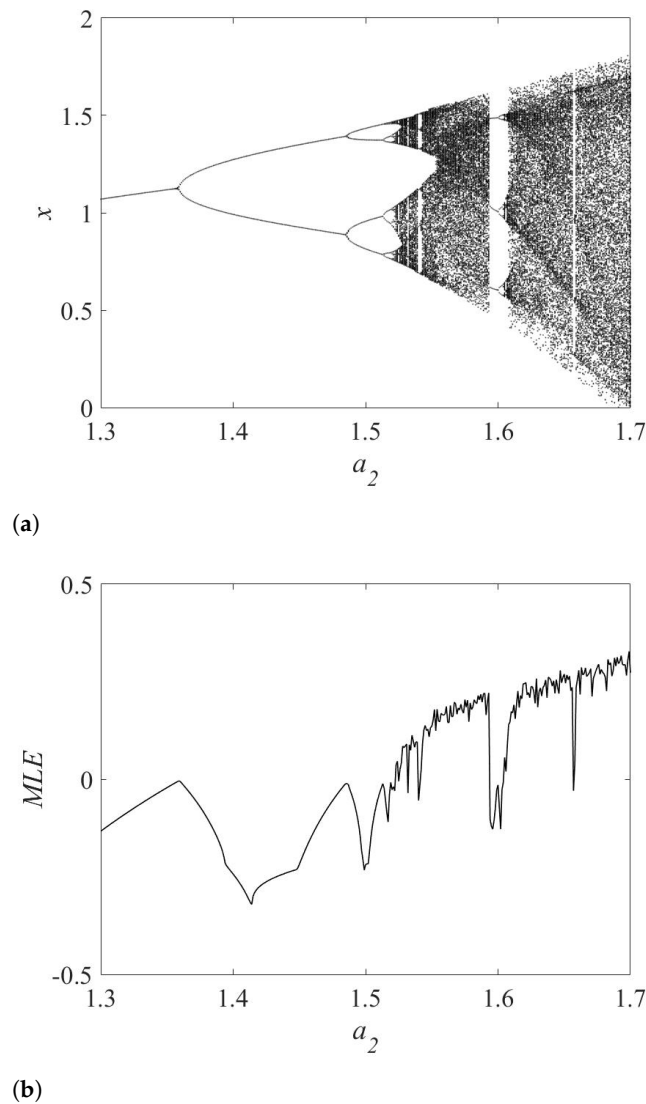


Figure 3. (a) Bifurcation diagram, (b) maximum Lyapunov exponents of the TDMM₁ map for $a_2 \in [1.3, 1.7]$.

The map is realized with a microcontroller via an Arduino Uno board. Signal x is displayed in Figure 4. The chaos of signal x verifies the map’s feasibility with hardware.

The Internet of Things (IoT) has emerged as a groundbreaking technology that promises to connect and automate various physical objects and devices, transforming industries and enhancing our daily lives. However, along with its numerous benefits, the IoT shows security challenges. The rapid proliferation of IoT devices, which are often embedded with sensors, actuators, and other smart technologies, has created a complex and interconnected network of devices that can be vulnerable to security threats. Lightweight cryptography plays a crucial role in securing IoT environments, where resource-constrained devices require efficient and effective cryptographic solutions [28,29]. Its ability to provide strong security with minimal resource requirements makes it suitable for a wide range of IoT applications, including secure communication, device authentication, data protection, access control, and secure firmware updates. As the IoT ecosystem continues to grow, the importance of lightweight cryptography in protecting IoT devices cannot be overstated. We test a simple lightweight encryption proposed by Moysis et al. [8] using the TDMM₁ map. In this simple encryption, we generate random numbers from the TDMM₁ map, which are utilized to encrypt a small-sized image via XOR operation. The encryption algorithm comprises the following steps.

Step 1: Formation of a secret key through the utilization of initial values and map parameters.

Step 2: Generation of a random bit sequence (K), with each bit (k_i) being generated by the map's state variable, x

$$k_i = \begin{cases} 1, & \text{if } \text{mod} \left(10^5 |x(i)|, 1 \right) \geq 0.5 \\ 0, & \text{if } \text{mod} \left(10^5 |x(i)|, 1 \right) < 0.5 \end{cases} \quad (7)$$

Step 3: Conversion of the original image into a binary sequence (P).

Step 4: Application of the XOR operation to yield the encrypted data (C): $C = P \oplus K$.

Step 5: Utilization of the XOR operation to derive the decrypted data (P'): $P' = C \oplus K$, allowing for the reconstruction of the original image.

The original, encrypted, and decrypted images are displayed in Figure 5. A uniform histogram of the encrypted image protects it against statistical attacks (see Figure 6). The information entropy calculations of the encrypted and original images are 7.9974 and 7.4509, respectively. The information entropy closer to 8 protects encrypted data against entropy attacks. The obtained results illustrate the possibility of the TDMM₁ map for use in lightweight encryption.

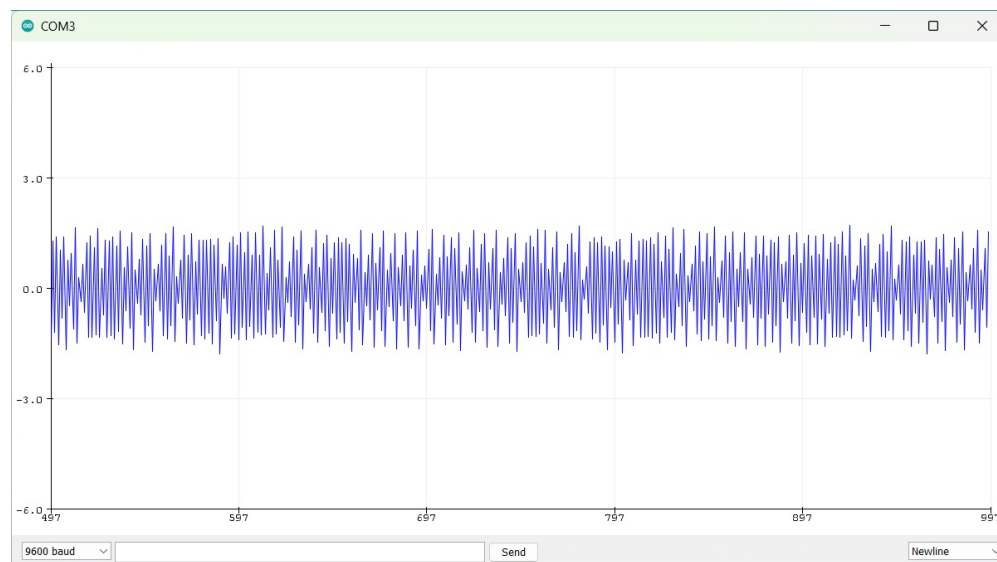


Figure 4. Experimental signal x captured by the Serial Plotter tool of Arduino.

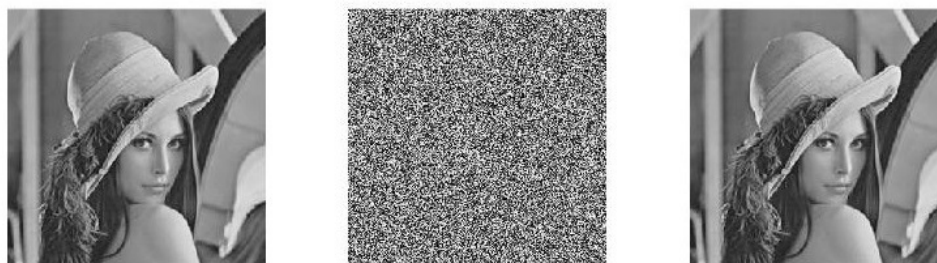


Figure 5. Obtained results: original image (left), encrypted image (middle), and decrypted image (right).

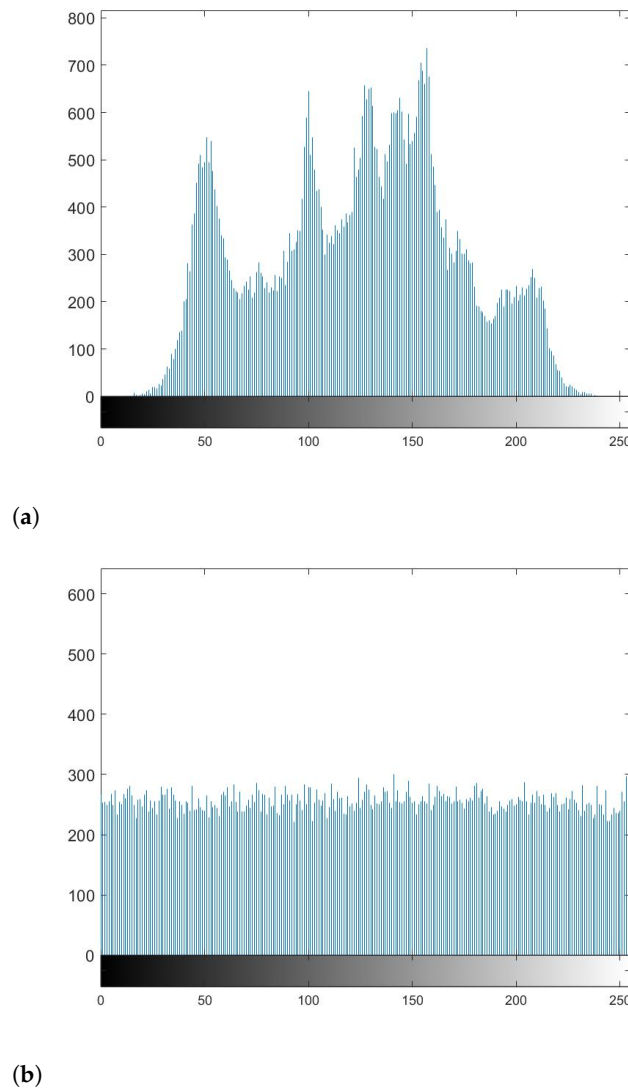


Figure 6. Histogram results of (a) original image and (b) encrypted image.

4. Discussion

High-dimensional chaotic maps, also known as multi-dimensional chaotic maps, are mathematical models that describe the dynamics of systems with many degrees of freedom. High-dimensional chaotic maps exhibit more complex and diverse behaviors than low-dimensional maps. By enlarging the model (1), higher-order dimensional maps are constructed easily.

Including an additional state $w(n)$ and $\sin(w(n))$, a 4D map is derived

$$\begin{cases} x(n + 1) = a_1 \sin(z(n)) + a_2 \sin(w(n)) + a_3((y(n))^2 - 1)x(n) + a_4 \\ y(n + 1) = y(n) + x(n) \\ z(n + 1) = a_5 \sin(z(n)) + a_6 x(n) \\ w(n + 1) = a_7 \sin(w(n)) + a_8 z(n) \end{cases} \tag{8}$$

with parameters $a_i, i = 1, \dots, 8$. The chaos in the 4D map is shown in Figure 7 for

$$\begin{cases} a_1 = a_2 = a_4 = a_5 = a_7 = 0.1 \\ a_3 = 1.7 \\ a_6 = 1 \\ a_8 = 0.2 \end{cases} \tag{9}$$

The value of MLE is 0.3003, confirming the presence of chaos.

Similarly, when introducing two states $w(n), v(n)$ and terms $\sin(w(n)), \sin(v(n))$, a 5D map is proposed as

$$\begin{cases} x(n+1) = a_1 \sin(z(n)) + a_2 \sin(w(n)) + a_3 \sin(v(n)) + a_4((y(n))^2 - 1)x(n) + a_5 \\ y(n+1) = y(n) + x(n) \\ z(n+1) = a_6 \sin(z(n)) + a_7 x(n) \\ w(n+1) = a_8 \sin(w(n)) + a_9 z(n) \\ v(n+1) = a_{10} \sin(v(n)) + a_{11} w(n) \end{cases} \tag{10}$$

with parameters $a_i, i = 1, \dots, 11$. Figure 8 displays the chaos in the 5D map for

$$\begin{cases} a_1 = a_2 = a_3 = a_5 = a_6 = a_8 = a_{10} = 0.1 \\ a_4 = 1.7 \\ a_7 = a_9 = 1 \\ a_{11} = 0.2 \end{cases} \tag{11}$$

The value of MLE is 0.2849.

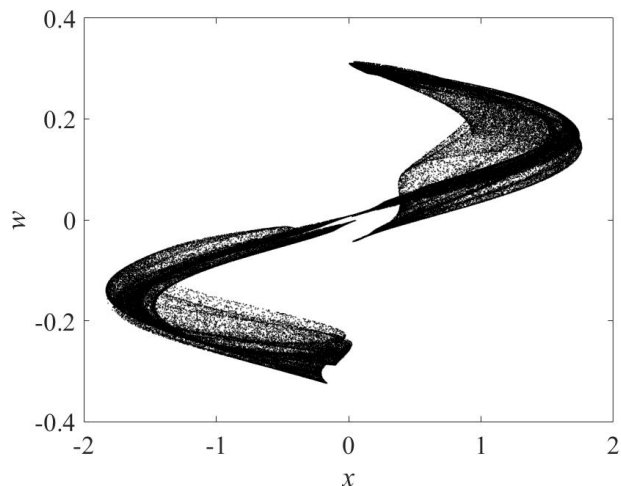


Figure 7. Iterative plots of the 4D map with $(x(0), y(0), z(0), w(0)) = (0.01, 0.01, 0.01, 0.01)$.

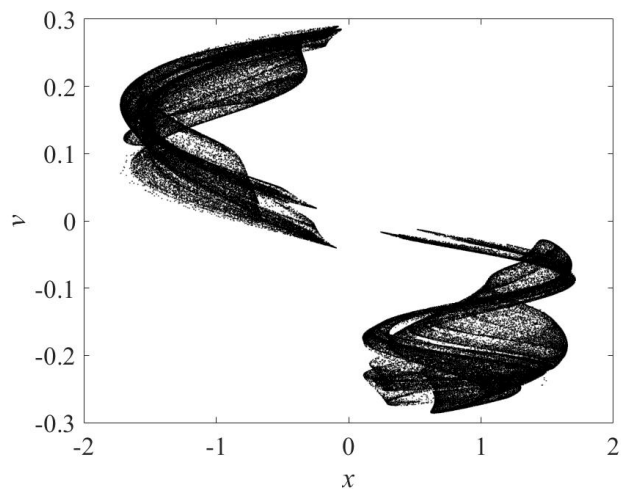


Figure 8. Iterative plots of the 5D map with $(x(0), y(0), z(0), w(0), v(0)) = (0.01, 0.01, 0.01, 0.01, 0.01)$.

5. Conclusions

We have conducted a study focusing on high-dimensional memristive maps, motivated by their potential application in various fields. In this research, we present a general approach to constructing these maps using memristors and sine terms. The resulting 3D model exhibits intriguing fixed points, making it particularly appealing. To illustrate the dynamics and practical applications of these maps, we specifically developed the TDMM₁ map, employing simulations and a microcontroller board. The TDMM₁ map generates chaotic signals, rendering it suitable for lightweight ciphers. Nevertheless, further investigations into the map's potential applications are planned for future work. In particular, the proposed approach is scalable and can be extended to create higher-dimensional maps, such as 4D and 5D maps.

Author Contributions: Conceptualization, G.G.; Investigation, O.A.A.; Methodology, V.-T.P.; Software, M.A.; Supervision, V.V.H.; Writing—original draft, S.A. All authors have read and agreed to the published version of the manuscript.

Funding: This research has been funded by the Scientific Research Deanship at the University of Ha'il, Saudi Arabia, through project number <<RG-23 087>>.

Data Availability Statement: No new data were created or analyzed in this study. Data sharing is not applicable to this article.

Conflicts of Interest: The authors declare no conflict of interest.

References

1. Pierre, C.; Jean-Pierre, E. *Iterated Map on the Interval as Dynamical Systems*; Springer: Berlin, Germany, 1980.
2. Dong, C.; Rajagopal, K.; He, S.; Jafari, S.; Sun, K. Chaotification of Sine-series maps based on the internal perturbation model. *Results Phys.* **2021**, *31*, 105010. [[CrossRef](#)]
3. Laskaridis, L.; Volos, C.; Munoz-Pacheco, J.; Stouboulos, I. Study of the dynamical behavior of an Ikeda-based map with a discrete memristor. *Integration* **2023**, *89*, 168–177. [[CrossRef](#)]
4. Zhu, W.; Sun, K.; He, S.; Wang, H.; Liu, W. A class of m-dimension grid multi-cavity hyperchaotic maps and its application. *Chaos Solitons Fractals* **2023**, *170*, 113370. [[CrossRef](#)]
5. Khennaoui, A.A.; Ouannas, A.; Bekiros, S.; Aly, A.A.; Jahanshahi, H.; Alsubaie, H. Hidden homogeneous extreme multistability of a fractional-order hyperchaotic discrete-time system: Chaos, initial offset boosting, amplitude control, control, and Synchronization. *Symmetry* **2023**, *15*, 139. [[CrossRef](#)]
6. Ali, Z.; Rabieli, F.; Hosseini, K. A fractal-fractional-order modified Predator-Prey mathematical model with immigrations. *Math. Comput. Simul.* **2023**, *207*, 466. [[CrossRef](#)]
7. Li, P.; Li, Y.; Xu, C.; Ren, J. Insight into Hopf bifurcation and control methods in fractional order BAM neural networks incorporating symmetric structure and delay. *Cogn. Comput.* **2023**, *preview*. [[CrossRef](#)]
8. Moysis, L.; Volos, C.; Jafari, S.; Munoz-Pacheco, J.; Kengne, J.; Rajagopal, K.; Stouboulo, I. Modification of the logistic map using fuzzy numbers with application to pseudorandom number generation and image encryption. *Entropy* **2020**, *4*, 474. [[CrossRef](#)]
9. Moysis, L.; Rajagopal, K.; Tutueva, A.; Volos, C.; Tekka, B.; Butusov, D. Chaotic path planning for 3D area coverage using a pseudo-random bit generator from a 1D chaotic map. *Mathematics* **2022**, *9*, 1821. [[CrossRef](#)]
10. Garcia-Grimaldo, C.; Bermudez-Marquez, C.F.; Tlelo-Cuautle, E.; Campos-Canton, E. FPGA implementation of a chaotic map with no fixed point. *Electronics* **2023**, *12*, 444. [[CrossRef](#)]
11. Bao, H.; Li, H.; Hua, Z.; Xu, Q.; Bao, B. Sine-transform-based memristive hyperchaotic model with hardware implementation. *IEEE Trans. Ind. Inform.* **2023**, *19*, 2792. [[CrossRef](#)]
12. Ma, M.; Lu, Y.; Li, Z.; Sun, Y.; Wang, C. Multistability and phase synchronization of Rulkov neurons coupled with a locally active discrete memristor. *Chin. Phys. B* **2023**, *32*, 058701. [[CrossRef](#)]
13. Bao, B.; Zhao, Q.; Yu, X.; Wu, H.; Xu, Q. Three-dimensional memristive Morris–Lecar model with magnetic induction effects and its FPGA implementation. *Cogn. Neurodynamics* **2023**, *17*, 1079. [[CrossRef](#)] [[PubMed](#)]
14. Bao, H.; Hua, Z.; Li, H.; Chen, M.; Bao, B. Memristor-based hyperchaotic maps and application in auxiliary classifier generative adversarial nets. *IEEE Trans. Ind. Inform.* **2022**, *18*, 5297–5306. [[CrossRef](#)]
15. Ma, M.; Xiong, K.; Li, Z.; Sun, Y. Dynamic behavior analysis and synchronization of memristor-coupled heterogeneous discrete neural networks. *Mathematics* **2023**, *11*, 375. [[CrossRef](#)]
16. Xu, Q.; Cheng, S.; Ju, Z.; Chen, M.; Wu, H. Asymmetric coexisting bifurcations and multi-stability in an asymmetric memristive diode-bridge-based jerk circuit. *Chin. J. Phys.* **2021**, *70*, 69–81. [[CrossRef](#)]
17. Bao, H.; Hua, Z.; Li, H.; Chen, M.; Bao, B. Discrete memristor hyperchaotic maps. *IEEE Trans. Circuits Syst. I Regul. Pap.* **2021**, *68*, 4534–4544. [[CrossRef](#)]

18. Zhao, Y.; Ding, J.; He, S.; Wang, H.; Sun, K. Fully fixed-point integrated digital circuit design of discrete memristive systems. *AEU-Int. J. Electron. Commun.* **2023**, *161*, 154522. [[CrossRef](#)]
19. Liu, X.; Sun, K.; Wang, H.; He, S. A class of novel discrete memristive chaotic map. *Chaos Solitons Fractals* **2023**, *174*, 113791. [[CrossRef](#)]
20. Wang, M.; An, M.; He, S.; Zhang, X.; Lu, H.H.C.; Li, Z. Two-dimensional memristive hyperchaotic maps with different coupling frames and its hardware implementation. *Chaos* **2023**, *33*, 073129. [[CrossRef](#)]
21. Sun, Q.; He, S.; Sun, K.; Wang, H. A novel hyperchaotic map with sine chaotification and discrete memristor. *Chin. Phys. B* **2022**, *31*, 120501. [[CrossRef](#)]
22. Wang, J.; Gu, Y.; Rong, K.; Xu, Q.; Zhang, X. Memristor-based Lozi map with hidden hyperchaos. *Mathematics* **2022**, *10*, 3426. [[CrossRef](#)]
23. Bao, H.; Gu, Y.; Xu, Q.; Zhang, X.; Bao, B. Parallel bi-memristor hyperchaotic map with extreme multistability. *Chaos Solitons Fractals* **2022**, *160*, 112273. [[CrossRef](#)]
24. Peng, Y.; He, S.; Sun, K. A higher dimensional chaotic map with discrete memristor. *AEU-Int. J. Electron. Commun.* **2021**, *129*, 153539. [[CrossRef](#)]
25. Zhang, L.; Liu, Y.; Wei, Z.; Jiang, H.; Bi, Q. Hidden attractors in a class of two-dimensional rational memristive maps with no fixed points. *Eur. Phys. J.-Spec. Top.* **2022**, *231*, 2173. [[CrossRef](#)]
26. Ramadoss, J.; Ouannas, A.; Tamba, V.K.; Grassi, G.; Momani, S.; Pham, V.T. Constructing non-fixed-point maps with memristors. *Eur. Phys. J. Plus* **2022**, *137*, 211. [[CrossRef](#)]
27. Bao, B.; Zhao, Q.; Yu, X.; Wu, H.; Xu, Q. Complex dynamics and initial state effects in a two-dimensional sine-bounded memristive map. *Chaos Solitons Fractals* **2023**, *173*, 113748. [[CrossRef](#)]
28. Gonzalez-Zapata, A.; Tlelo-Cuautle, E.; Cruz-Vega, I.; Leon-Salas, W. Synchronization of chaotic artificial neurons and its application to secure image transmission under MQTT for IoT protocol. *Nonlinear Dyn.* **2021**, *104*, 4581. [[CrossRef](#)]
29. Trujillo-Toledo, D.; Lopez-Bonilla, O.; Garcia-Guerrero, E.; Tlelo-Cuautle, E.; Lopez-Mancilla, D.; Guillen-Fernandez, O.; Inzunza-Gonzalez, E. Real-time RGB image encryption for IoT applications using enhanced sequences from chaotic maps. *Chaos Solitons Fractals* **2021**, *153*, 111506. [[CrossRef](#)]

Disclaimer/Publisher's Note: The statements, opinions and data contained in all publications are solely those of the individual author(s) and contributor(s) and not of MDPI and/or the editor(s). MDPI and/or the editor(s) disclaim responsibility for any injury to people or property resulting from any ideas, methods, instructions or products referred to in the content.